Journal of Pharmacy and Pharmacology 6 (2018) 175-187
doi: 10.17265/2328-2150/2018.02.011

A Simple Procedure to Fabricate Paper Biosensor and Its Applicability—NADH/NAD^+ Redox System

Isabel Ribau and Elvira Fortunato

Departamento de Ciências dos Materiais, Faculdade de Ciências e Tecnologia, Universidade Nova de Lisboa, Campus de Caparica, Caparica 2829-516, Portugal

Abstract: A simple device which incorporates three electrodes (working electrode, counter electrode and reference electrode) was constructed to be used currently in laboratories without elevated cost. It does not need more than 2 μL of electrolyte, sample or working solution, his support material is paper, and the working electrode which is based on carbon ink can incorporate enzymes and cofactors. To test this concept we started this investigation using the NADH/NAD^+ redox couple which is an omnipresent coenzyme in living systems but is also a challenge to electrochemistry. The paper sensor fabrication was simple, rapid and cheaper. NADH was incorporated in the carbon ink by mixing both and, this mixture was used to print the working electrode. The direct electrochemical system NADH/NAD^+ signal obtained, using this device, appeared at low potentials. A quasi-reversible diffusional redox process was achieved and regeneration of the NADH after oxidation was reached. This small paper device was not only used to study the redox process of NAD^+/NADH, but also its behavior in the presence of electroactive (ascorbic acid) and non-eletroactive species (glucose).

Key words: NADH/NAD^+, screen-printing biosensor, paper device.

1. Introduction

The redox system NADH/NAD^+ has been very important in nature, not only because it is a ubiquitous coenzyme, but also because it participates in many cellular reactions. This system is important in pharmaceutical and food industry as well as in biotechnology industry since it is present in drugs, biosensors, but also in biofuel cells and bioreactors [1-7], nevertheless is expensive and the redox process is usually irreversible [3, 6].

In the NAD^+ reduction, the reversible redox process occurs in nicotinamide ring, which accepts two electrons from a substrate in the presence of an appropriated enzyme, forming NADH: $SH_2 + NAD^+ \rightleftarrows S + NADH + H^+$ [3]. This reaction is particularly important since it allows the identification of non-eletroactive substrates that interact with NAD^+ and take part in its reduction [8].

NADH molecule can be oxidized through the nicotinamide or adenosine groups [8]. The NADH is able to oxidize at potential higher than +0.4 V (Ag/AgCl) on carbon paste electrodes [3, 8]. Adenosine free in solution is oxidized at +1.2 V (vs. SCE, pH 7.0) in carbon electrodes. Nicotinamide presents an oxidation peak at +0.45 V (vs. SCE, pH 7.0) in carbon electrodes. In the same conditions the peak at +1.05 V was attributed to the formation of an adduct between phosphate anions and NADH through adenine and nicotinamide groups. If in phosphate medium, using a glassy carbon electrode, a potential higher than +0.9 V is applied to nicotinamide, it promotes the surface blocking with adducts [8].

The oxidation of NADH in bare electrodes occurs via radical cation intermediates, which may lead to the fouling process and surface poisoning with the formation of inactive NAD_2 dimers (adsorbed on the electrode surface), adducts or the formation NADH (active form). As a result of these reactions, low sensitivity, selectivity and stability are achieved [3, 5, 8, 9].

Some research has been done to study the direct

Corresponding author: Isabel Ribau, Ph.D., researcher, research fields: biosensors and bioeletrochemistry.

electrochemistry of NAD^+/NADH and the possible causes of the reduction irreversibility, with the formation of inactive form NAD_2 reported in some studies [6, 8, 10]. In one of these researches, it was possible to regenerate NAD^+ to the active form, 1,4-NADH, applying a regeneration potential [6]. The reduction reaction of NAD^+ on glassy carbon was irreversible and under diffusion control, at a formal potential, $E^{0'}$ (NAD^+/NADH) = -0.885 V (pH 5.8). In another article the formal redox potential of NAD^+/NADH was -0.560 V (vs. SCE), or -0.315 V (vs. NHE, pH 7) and the $E^{0'}$ variation with pH was -30.3 mV/pH [5]. For a reversible process, in unmodified carbon surfaces, the formal potential of the redox coupled NAD^+/ NADH was -0.32 V (NHE, pH 7) but the heterogeneous kinetic was slower and interferences could occur [3, 6]. Using different electrochemical techniques, the apparent formal heterogeneous electron-transfer rate constant was estimated as $(6.1 \pm 2) \times 10^{-14}$ cms^{-1} and $(2.5 \pm 1) \times 10^{-14}$ cms^{-1} [6]. These low values indicate very slow kinetics of the NAD^+ reduction reaction on a glassy carbon electrode and reflect the over potential necessary for the redox reaction which is related to both redox kinetics and mass transport.

One strategy employed to overcome these difficulties (fouling and overvoltage and side reactions) was the use of mediator-modified electrodes, where the mediators are used to shuttle electrons from NADH to the electrode surface and allow electron transport between them [5, 9-16]. Some mediators (electrocatalysts) were immobilized on the electrode surface by covalent attachment, electrochemical polymerization, incorporation in carbon paste, adsorption, self-assembly and via entrapment in polymeric matrices [4, 17-19]. Another strategy is modification of the electrode surface with a polymeric substance, using electrodes modified with carbon nanotubes, nanofibers or using enzymatic methods that follow bioelectrocatalytic reaction [2, 4, 13, 15, 16, 20-23]. Investigation in this area usually explores the mediator use or the surface modification to improve the electrochemical detection [15, 21, 24-28]. Some literature has been published related to the study of the redox couple NADH/NAD^+ in screen printing electrodes [1, 4, 21, 24-27, 29-34]. The sensor built using this technique can incorporate the three electrodes (working electrode, reference and counter electrode), can be easily produced and miniaturized, work with a minimum volume (2 μL), it needs low reagent consumption, it can be fabricated in many supports (paper, glass) and sensors are disposable devices that can be used in many science fields [26, 35]. In a screen-printing electrode prototype, the oxidation of NADH (0.4 mM) occurred in a potential range from +0.18 V to +0.44 V but the signals were not well-defined [34]. At a screen-printing electrodes modified with MWCNTs (multiwalled carbon nanotubes), or AuNPs (gold nanoparticles) or with PNRs (polyneutral red films), it was possible to verify that the best response of the redox system NAD^+/NADH was obtained with the modification using MWCNTs, which was used as an amperometric NADH detector [27].

The goal of this report is to present a sensor that can be easily fabricated, which is cheaper and environmentally friend and allows the electrochemical study of the redox couple NADH/NAD^+. With this aim, we present an NADH/ NAD^+ biosensor, for sensing subtracts that can interact with the cofactor.

There are significant advantages of using this biosensor, the first is that it is possible to obtain the oxidation and reduction peak of the redox couple NADH/NAD^+ in lower potentials, second is the possibility to sense either electroactive as non-electroactive species, the third is that the fabricated device is not time-consuming (is quick and simple), the fourth is the low cost of the device, the fifth is the ecological approach as this device is made with paper.

2. Material and Methods

2.1 Materials

All reagents used were of analytical grade β-nicotinamide adenine dinucleotide, NADH (reduced disodium salt hydrate), β-D-glucose, ascorbic acid, potassium chloride and potassium ferrocyanide were acquired from Sigma-Aldrich. All solutions were prepared with buffer. All buffers used in this work were commercial and purchased from ROTH (Germany). The electrolyte was a buffer solution with potassium chloride (0.1 M).

2.2 Fabrication of the Biosensors

The fabrication procedure that will be described below, is not time consuming (it takes 15 minutes to do 5 biosensors), is low cost (the price is lower than 0.2 Euros per electrode) and is ecological (the biosensors is constructed with paper, and the silver and carbon ink can be removed and recovered).

The carbon ink and Ag/AgCl ink were purchased from Conductive Compounds. The working electrode was of carbon ink which was added to the solid β-nicotinamide adenine dinucleotide (see Section 2.3 Working Electrode Preparation).

A Xerox Color Qube 8570 printer was used to print the hydrophobic region of the devices. The paper used was Whatman n.^{0} 1 chromatographic paper, and the wax was obtained from Xerox. After the wax printing, the wax was heat treated during 10 s in a hot plate (150 ^{o}C). After that, the paper, cooled at room temperature, was ready to perform the screen printing technique. The configuration system design was a three-electrode system with an Ag/AgCl as the reference electrode, a carbon counter electrode and a working electrode based on carbon ink, Figs. 1A and 1B.

The counter electrode was printed with conductive carbon ink, which was deposited above the hydrophobic matrix (wax). Then the mesh was removed and the device was allowed to heat at hot plate

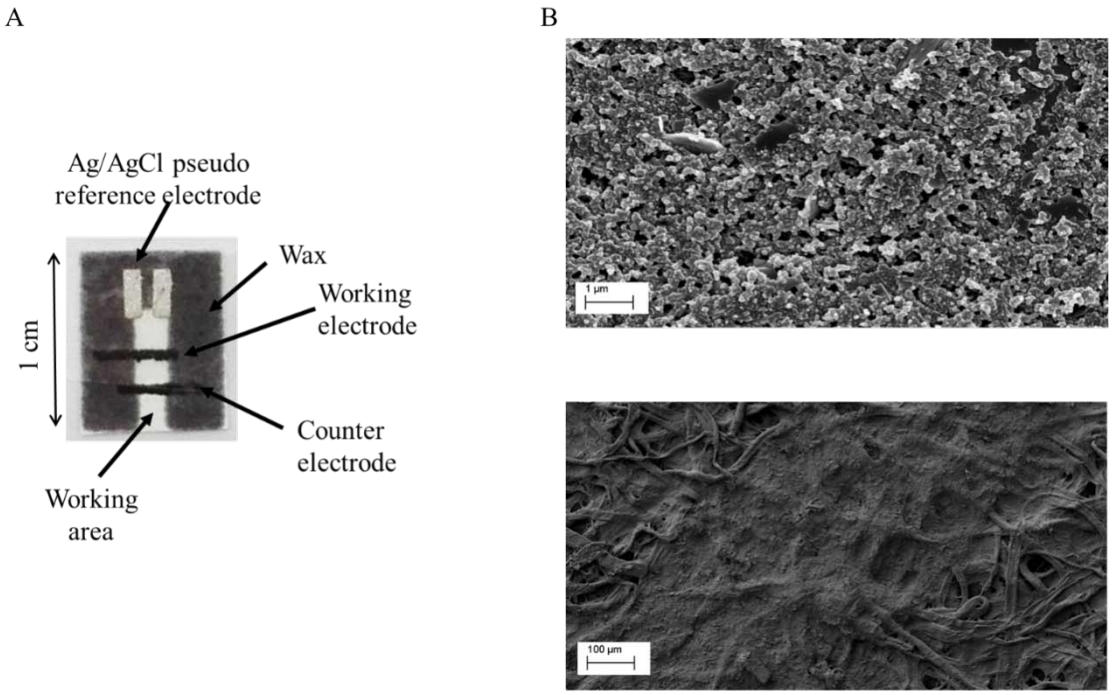

Fig. 1 Biosensor with a three-electrode configuration system design with an Ag/AgCl reference electrode, a carbon counter electrode and a working electrode based in carbon ink (A). SEM (scanning electron microscopy) images of the working electrode surface (B). Upper image scale is 1 µm, and down image scale is 100 µm. Observations were carried out using a Carl Zeiss AURIGA Cross Beam (FIB-SEM) workstation coupled with energy dispersive X-ray spectroscopy (EDS) from Oxford Instruments. The materials have been previously coated with an Ir conductive film for avoiding charge effects.

(60 ^oC) during 5 minutes. Once the construction of the counter was concluded, the working electrode was printed and dried the same way as described before. The reference electrode, fabricated with Ag/AgCl ink had the same screen printing treatment.

2.3 Working Electrode Preparation

A mixture with the cofactor (NADH) enclosed in the carbon ink was prepared and used to make the working electrode.

2.4 Electrochemical Detection

During the electrochemical measurements, a drop of the interest solutions (2 μL) was spotted in the hydrophobic channel between the wax-limited zones (working area) and it was dispersed through the paper matrix in a few seconds, being in contact with the three electrodes. The electrochemical behavior of each biosensor was experimentally characterized through cyclic voltammetry.

All electrochemical acquisitions and measurements were performed in a Gamry ESA419 data acquisition system, using PHE 200 physical electrochemical and PV 220 physical electrochemical software coupled with a Gamry instruments (reference 600) potentiostat/galvanostat (ZRA) and the data analysis was processed by Gamry software package. All the experimental procedures were performed in normal atmosphere in the presence of oxygen.

3. Results and Discussion

The electrochemical behavior of the redox couple NAD$^+$/NADH has been analyzed in the last years due to its role as a cofactor, and as an electron carrier in living organisms [5, 6, 14].

In this research work the cofactor electrochemical behavior was studied using the PBS buffer (pH 7) with KCl (0.1 M) as the electrolyte. This pH was chosen because NADH is instable in highly alkaline and acidic solutions due to its rapid degradation [27].

3.1 Electrode Surface Area

The electrochemical characterization of the electrodes was made using the standard heterogeneous rate constant (k^0) and the effective electroactive area.

To obtain the electrode real surface area, a redox model par, potassium ferri(III)cyanide/ ferro(II)cyanide, $K_3/K_4Fe(CN)_6$, was used. The cyclic voltammograms were recorded in the sweep between 20 mV·s^{-1} and 150 mV·s^{-1} in PBS buffer (pH 7) with 100 mM KCl as the supporting electrolyte. From these recordings, the peak currents were measured, in Fig. 2.

The peak potential average of the reduction and oxidation, $E_{1/2}$, is related to the formal potential $E^{0'}$ by Eq. 2, $E_{1/2} = E^{0'} + (RT/nF)1\ ln(D_r/D_o)$. As the diffusion coefficient is related to the peak current vs. scan rate square root slope, D_r/D_o is approximately one and $E_{1/2} = E^{0'}$. The formal reduction potential can be estimated from the average of the reduction and oxidation peak potentials and a value of $E^{0'} = (E_p^c + E_p^a)/2$.

The results presented are the medium values obtained with two screen-printed electrodes: (E_p^a = (+269 ± 1) mV vs. Ag/AgCl; E_p^c = (+163 ± 6) mV vs. Ag/AgCl), a midpoint, $E^{0'}$, of (+216 ± 3) mV vs. Ag/AgCl, and peak separation of (+107 ± 7) mV vs. Ag/AgCl. Peak currents vary linearly with the square root of the scan rate, in the studied rate range, thus denoting a diffusion controlled process.

The peak currents ratio obtained in these experiments ($|i_p^a/i_p^c|$ = +0.72 ± 0.05), and the peak to peak separation enable us to conclude that in these conditions the potassium ferri(III) cyanide /ferro (II) cyanide do not present a reversible behavior as it was expected. It is possible to verify that the ratio $i_p/v^{1/2}$ is independent of the scan rate (in the range between 150 mV·s^{-1} and 20 mV. s^{-1}), $i_p^a/v^{1/2}$ (+29.1 ± 1.2) μA and $i_p^c/v^{1/2}$ (-20.8 ± 1.3) μA, but E_p varies with the scan rate and ΔE_p also increases with the scan rate indicating that in these conditions the redox par behaves like a quasi-reversible system.

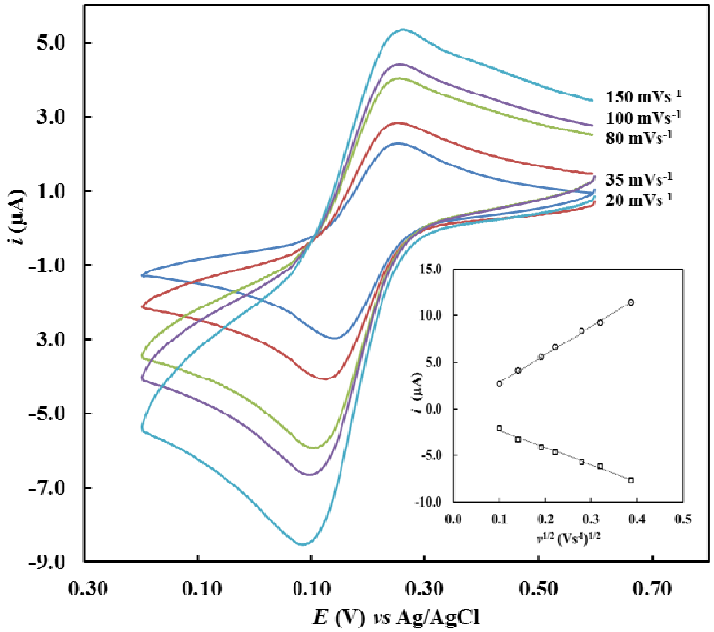

Fig. 2 Cyclic voltammograms ($E_i = E_f$ = +0.6 V, $E_{inversion}$ = -0.2 V) (E_d = -0.5 V) at a screen at a screen printing electrode with a three-electrode system configuration with an Ag/AgCl reference electrode, a carbon counter electrode and a working electrode with NADH (reduced form disodium (35 mg)) in carbon ink (800 mg) in the presence $K_3Fe(CN)_6$ (1 mM) of PBS (7.0) with KCl (0.1 M). Insertion: Variation of the anodic and cathodic peak current with the square root of the sweep rate. The better fit equation is: (⁘) $i_p^a = 29.974\ v^{1/2} - 0.1463R^2 = 0.9976$; (□) $i_p^c = -18.419\ v^{1/2} - 0.4838R^2 = 0.9911$.

The electrochemical reversibility can be evaluated using the rate of heterogeneous electron transfer standard constant (k) [36, 37]. When the k presents low values, the electron transfer kinetics are slow, but if it is high it indicates fast electron transfer kinetics. In these analyses, to determine the heterogeneous electron transfer constant, we used the method developed by Nicholson [36, 37]. The transfer coefficient value, α, can be accessed by comparing experimental curves with the theoretical ones. ΔE_p is independent of α in the range 0.3 to 0.7, which allowed the determination of k, without knowing these parameters. In these intervals of α, there is a relation between ΔE_p and the kinetic parameter ψ (Eq. 1, $\psi = \gamma^{\alpha} k/\sqrt{(\pi a D_o)}$, where $\gamma = (D_o/D_r)^{1/2}$, $a = nFv/RT$ when $\alpha = 0.5$), which is used to calculate the k. Using for D_o (diffusion coefficient for ferri cyanide) the value 7.6×10^{-6} cm^2·s^{-1}, and for D_r (diffusion coefficient for ferrocyanide) the value 6.5×10^{-6} cm^2·s^{-1} and a transfer coefficient value of 0.5, it was possible to find the heterogeneous electron transfer constant, k, of $(2.63 \pm 0.46) \times 10^{-2}$ cm·s^{-1}. This value is bigger than the value found in other studies with screen-printing electrodes (5.2×10^{-6} cm·s^{-1}) [1] and indicates that we are in the presence of a quasi-reversible system.

To estimate surface area the Randles-Sevčik equation was used, in a range between 20 mV·s^{-1} and 150 mV·s^{-1}. From the slope of the i_p vs. $v^{1/2}$ plots it was possible to calculate the medium active area as 3.5 ± 0.7 mm^2. The Randles-Sevčik equation, $i_p = (2.69 \times 10^5) n^{3/2} A D^{1/2} c v^{1/2}$, (where n is the number of electrons exchange in the redox process, here n = 1; A is the electrochemically active electrode area in cm^2; c is the concentration of the electric species in mol/cm^3; v is the scan rate (V/s) and D is the diffusion coefficient in cm^2/s), was used to estimate the effective electrode surface area (3.5 mm^2) and it was obtained from Randles-Sevčik equation, through the parameters obtained for potassium ferrocyanide/ferricyanide redox system [38].

After five months the electrode area was determined again, using biosensors that were stored in

the laboratory, without the humidity control, in Fig. 3. The biosensors were made in the winter, and now it was summer.

Some parameters were examined. The variation of the anodic and cathodic peak current with the square root of the sweep rate was analyzed. A cathodic peak, E_p^a = (+232 ± 4) mV and an anodic peak, E_p^c = (+160 ± 7) mV are observed, and a separation of anodic to cathodic peak, Δ*E*p, with a value of (+78 ± 15) mV vs. Ag/AgCl was obtained and a formal potential of $E^{0\prime}$ = (+192 ± 4) mV vs. Ag/AgCl was calculated. A ratio of anodic to cathodic peaks current, $|i_p^a/i_p^c|$ = +0.84 ± 0.04. A linear variation of the current peak with the scan rate square root is obtained: i_p^a = 7.686$v^{1/2}$-0.3395 μA, R^2 = 0.9974, i_p^c = -5.928 $v^{1/2}$ + 0.188 μA, R^2 = 0.99. The Randles-Sevčik equation $i_p = (2.69 \times 10^5)n^{3/2}AD^{1/2}cv^{1/2}$), was used to estimate the active area after five months storage, and in these conditions the active area was (0.98 ± 0.09) mm^2. The heterogeneous electron transfer standard constant (k) calculated is (3.78 ± 0.18) ×10^{-5} cm·s^{-1}. The active area reduction was almost 75%. So storing these electrodes at room temperature, without any special care (humidity control) is not a good solution, so they must be produced and used in a short time or stored in controlled conditions (humidity and temperature). This result also focuses our attention on the necessity of having good hydrophilicity of the electrode surface to have a major active area.

3.2 NADH Responses in Screen Printing Electrodes

The direct electro oxidation of NADH, and the reduction of NAD$^+$, (NADH ⇄ NAD$^+$ + H$^+$ + 2ē) was analyzed using the screen-printing electrodes fabricated as described above. To obtain stable NADH signals it was applied, previously to each measure, a potential of -0.5 V during 5 seconds, and CVs (cyclic voltammograms) were recorded in the electrolyte (PBS buffer solution pH 7 with KCl (0.1M)). The scan was initialized in -0.4 V to +0.4 V and the reverse reduction was carried out. Two well-defined peaks appear in the cyclic voltammograms. These peaks can be assigned to

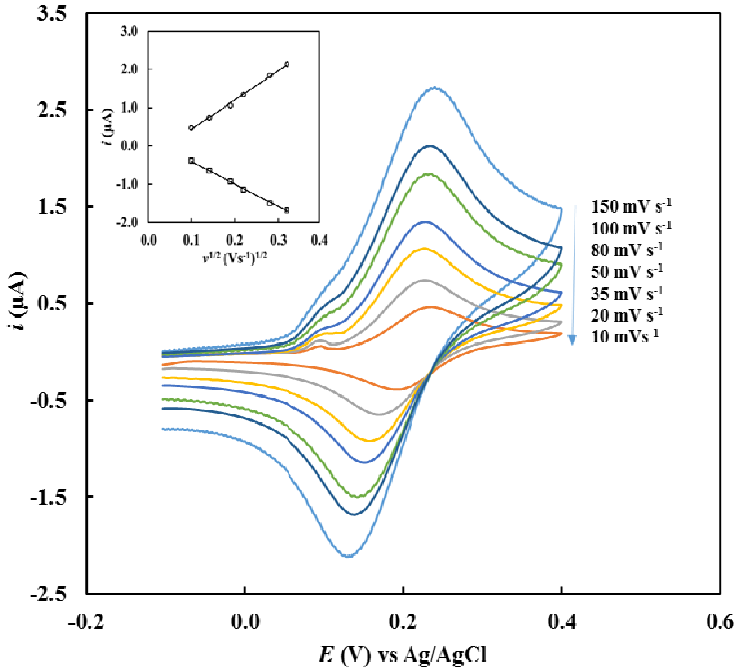

Fig. 3 Cyclic voltammograms (E_i = E_f = +0.2 V, $E_{inversion}$ = +0.4 V) (E_d = -0.5 V) at a screen printing electrode with a three-electrode system configuration with an Ag/AgCl reference electrode, a carbon counter electrode and a working electrode with NADH (reduced form disodium (35 mg)) in carbon ink (800 mg) in the presence $K_3Fe(CN)_6$ (2 mM) of PBS (7.0) with KCl (0.1M),. Insertion: Variation of the anodic and cathodic peak current with the square root of the sweep rate. The best fit equation is: (∴) i_p^a = 7.686 $v^{1/2}$ - 0.3395, R^2 = 0.9976; (□) i_p^c = -5.928 $v^{1/2}$ + 0.188, R^2 = 0.9911.

NADH oxidation and NAD$^+$ reduction, once there were not another species in the device. Some articles report the same positive potential value obtained during the NADH oxidation process on a bare glassy carbon electrode [8] using carbon nanofibers modified glassy carbon electrodes [23]. But the reduction peak, which is observed in this experiment, was not shown or analyzed in those articles.

Our data reveal a scan rate dependent behavior. In scan rate between 15 mV and 100 mV·s^{-1}, peak currents vary linearly with the square root of the sweep rate, indicating a diffusion controlled process. In this condition a cathodic peak, E_p^a = (105.0 ± 6.0) mV vs. Ag/AgCl and an anodic peak, E_p^c = (-125.0 ± 25.0) mV vs. Ag/AgCl are observed. The anodic and cathodic peak separation, ΔE_p, presented a value of (230.0 ± 30) mV vs. Ag/AgCl and a formal potential of $E^{0'}$ = (-10.0 ± 10) mV vs. Ag/AgCl was achieved. For small scan rates (15 mV·s^{-1} < v < 100 mV·s^{-1}) the transport system was governed by diffusion, in Fig. 4A, but for scan rates higher than 150 mV·s^{-1} it was thin layer, in Fig. 4B.

At high scan rates (600 mV·s^{-1}> v > 150 mV·s^{-1}) NADH behaves in this screen-printing electrode as a quasi-reversible system. Peak currents vary linearly with the sweep rate with a null intercept. The peak-to-peak separations, E_p^a-E_p^c, remain almost constant with *v*, and equal to (289 ± 15.0) mV vs. Ag/AgCl, and the midpoint potential is (-42.0 ± 4.0) mV vs. Ag/AgCl. This behavior indicates that the voltammetric response arises from a diffusionless redox process in which both oxidized and reduced forms are adsorbed.

In literature it is reported that the NADH nicotinamide ring undergoes a two-electron oxidation producing NAD$^+$, in aqueous medium and in carbon paste electrodes, at anodic potentials higher than 0.4 V (vs. Ag/AgCl). Although the formal potential for

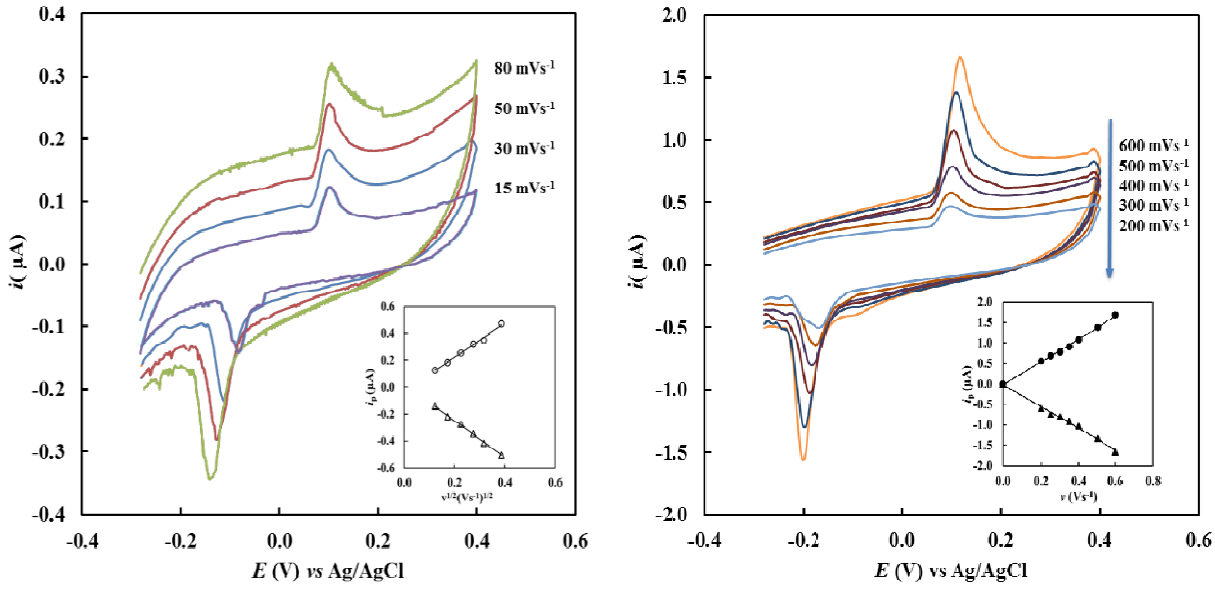

A B

Fig. 4 Cyclic voltammograms of NADH oxidation (E_i = E_f = +0.4 V, $E_{inversion}$ = -0.4 V) at a screen at a screen printing electrode with a three-electrode system configuration with an Ag/AgCl reference electrode, a carbon counter electrode and a working electrode with NADH (reduced form disodium (35 mg)) in carbon ink (800 mg) in PBS (7.0) with KCl (0.1M), after a potential application ($E_{application}$ = -0.5 V) during 5 s. (A) 15 mV·s^{-1} < v < 80 mV·s^{-1} Insertion: variation in the CV cathodic and anodic peak current with the square root scan rate. The best fit curve are (○) i_p^a = 1.2775 v$^{1/2}$ - 0.035, R² = 0.9928; (Δ) i_p^c = -1.373 v$^{1/2}$ + 0.0264, R² = 0.9981. (B) 200 mV·s^{-1} < v < 600 mV·s^{-1}. Insertion: variation in the CV cathodic and anodic peak current with the scan rate. The best fit curves are (●) i_p^a = 2.789v - 0.0412, R² = 0.9952, (▲) i_p^c = -2.5849v - 0.0493, R² = 0.984.

NAD^+/NADH is -0.32 V (NHE) at pH 7 (25ºC) or -0.56 V (SCE) [5], literature refers that it is necessary for high potentials to use mediators to achieve appropriated electron transfer kinetics [20]. With this electrode it was possible to reach a formal potential of near +0.250 V vs. NHE, without modification or surface treatments.

For a reversible system controlled by diffusion, $\Delta E_p = 59/n$ (n is the electron exchange number). In this case, ΔE_p is bigger than the theoretical value for an oxidation involving two electrons (Eq. 2) and it is related with nature of the electrode (sensor is a screen printing electrode where the NADH is inner and above the surface) which has a heterogeneous surface that has holes, fissures, grooves and different hydration degrees, but also different surface groups which implies environmental changes [39]. Comparing this value with the literature, the peak-to-peak variation is similar to the data reported by other authors when used screen printing electrodes [30, 39, 40]. In screen-printing electrodes a ΔE_p of (+229 ± 2) mV was reported for the redox couple $[Fe(CN)_6]^{4-}/[Fe(CN)_6]^{3-}$ known as a reversible system [30]. The authors interpreted this result, based on the fact that a rather slow electron transfer occurs due to the composition of the graphite ink. So this ink does not have the ideal characteristic to be used in amperometric devices.

In Fig. 5, it is possible to see the variation in the logarithm of the cathodic and anodic CV peaks with the logarithm of the scan rate.

Two linear portions appear with different slopes: a slope close to 0.5 for scan rates 15 $mV \cdot s^{-1} < v < 100$ $mV \cdot s^{-1}$ and a slope that tends to one for higher scan rates. These findings corroborate a redox system in which two mechanisms are operating: mainly a diffusion-controlled one for lowest scan rates, and oxidation from an adsorbed state for highest scan rates [36, 38, 41]. For higher scan rates, oxidation from the adsorbed state seems to predominate over the diffusion process. This double mechanism is related to the nature of the electrode (the working electrode is a screen printing electrode where the NADH is inner and above the surface). For slow scan rate, some NADH molecules that are near the electrode surface, and are in contact with the electrolyte, can migrate from the electrode to the buffer solution by diffusion; for fast sweep rates only the NADH molecules that are in the surface of the electrode and in direct contact with the solution can suffer oxidation behaving as a thin layer.

In the case of quasi-reversible systems, the electron transfer mechanism is not only controlled by diffusion, but it is also related to the kinetics process. Using the redox system ferrycyanide/ferrocyanide, it was possible to determine the effective electrode area (3.5 mm^2) and the heterogeneous constant velocity as (2.63 ± 0.46) × 10^{-2} $cm \cdot s^{-1}$ (see section 3.1 Electrode Surface Area). These values indicate that the electron transfer between the electrode surface and the ferrycyanide/ferrocyanide is slow. But it is higher than the value found in other

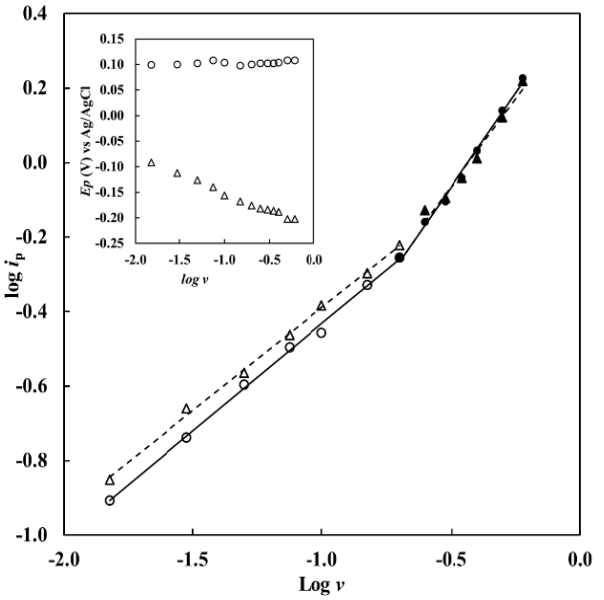

Fig. 5 Variations in the logarithm of CV cathodic and anodic peak current with the logarithm of the scan rate of the cyclic voltammograms of NADH oxidation in buffer. The best-fit curve are (○) log i_p^a= 0.5748 log$v$ + 0.1419, R^2 = 0.9973 and (Δ) log i_p^c = 0.5511 log$v$ + 0.1619, R^2 = 0.9983, for 15 $mV \cdot s^{-1} < v < 100$ $mV \cdot s^{-1}$. For 150 $mV \cdot s^{-1} < v < 600$ $mV \cdot s^{-1}$ (●) log i_p^a = 1.098 log$v$ + 0.4387, R^2 = 0.994 and (▲) i_p^c = 0.936 log$v$ + 0.405, R^2 = 0.9732. Insertion: Variation in the cathodic and anodic CV peak potentials with the v logarithm.

studies with screen-printing electrodes (5.2×10^{-6} cm·s^{-1}) [29].

In both amperometric biosensors and biofuel cells an efficient regeneration of NADH/NAD$^+$ is required. In this context we developed a system that allowed the regeneration of both species. It is necessary to use another carbon ink to increase electron transfer velocity between the electrode surface and the redox system.

A new set of experiments was carried out, using six different electrodes, in low scan rate between 10 mV·s^{-1} and 150 mV·s^{-1}, to analyze the persistence and the reproducibility of the signal. The anodic and cathodic current peak varies with the square root of the sweep rate, thus denoting the predominance of diffusion controlled process [36, 38]. A cathodic peak, E_p^a = (+82 ± 4) mV and an anodic peak, E_p^c = (-159 ± 2) mV is observed, and a separation of anodic to cathodic peak, ΔE_p, with a value of (+221 ± 2) mV vs. Ag/AgCl was obtained and a formal potential, $E^{0'}$, of (-38 ± 1) mV vs. Ag/AgCl was calculated. But a ratio of anodic to cathodic peaks current, $|i_p^a/i_p^c|$ estimated was far from unit. In this condition NADH behaves as a quasi-reversible system. A linear variation of the current peak with the scan rate square root is obtained: $i_p^a = 1.0946\ v^{1/2}$-0.035 μA, R = 0.99, $i_p^c = -1.777\ v^{1/2}$ + 0.0803 μA, R = 0.99, in Fig. 6.

It is possible to observe that the cathodic peak presents more variation than the anodic peak, and that for the smallest scan rate the variation is almost null. This may be related to the reduction process and to the appearance of some interferent species that have a rapid kinetics as the dimer. But the potential application before each voltammogram may reduce this interferent species, allowing the reduction of NAD$^+$ to NADH in slow scan rate.

In a research using a PPS-modified carbon electrodes (poly(phenosafranin)-modified carbon electrodes) the regeneration of NADH/NAD$^+$ was possible and the formal potential value found was (-365 ± 2) mV vs. SHE, pH 7.0 [9]. Comparing this result with ours ((-38 ± 1) mV vs. Ag/AgCl, pH 7), it is possible to verify that with our strategy, the results are similar.

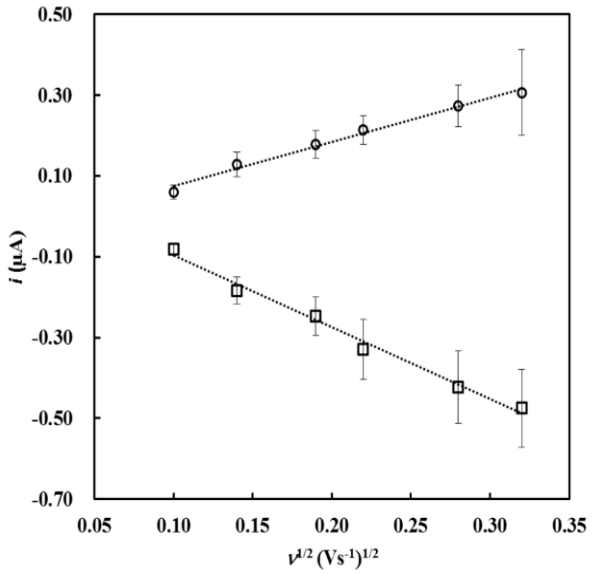

Fig. 6 Variations of the anodic and cathodic peak current with the square root of the sweep rate, in pH 7. The better fit equation is: (⁘) $i_p^a = 1.0946\ v^{1/2}$ - 0.035, R^2 = 0.988, n = 6; (□) $i_p^c = -1.777\ v^{1/2}$ + 0.0803, R^2 = 0.9893, n = 6 (six measures which implied six different biosensors).

A diffusion coefficient for the system NADH/NAD$^+$ could not be estimated from the experimental data, because its concentration is unknown. In fact, the NADH/NAD$^+$ diffusion occurred initially from the electrode surface to the electrolyte solution, and it was governed by gradient concentration.

The pH dependence of the redox potential of NADH/NAD$^+$ was also analyzed. At pH from 3 to 9 the redox potential average, the formal potential was (-33 ± 4) mV. This result is not similar to the reported in literature, which refer a dependence of -30.3 mV/pH. The stability of the formal potential may be related to the initial reduction on the electrode surface [5, 32].

3.3 Influence of Nonelectroactive and Electroactive Species in the NADH/NAD$^+$ Redox System Responses

The presence of some molecules presented in living organism was studied with this sensor. The effect of the glucose, a non electroactive species, was analyzed, in pH 7. At a neutral pH, glucose in the range of 2-15 mM, promotes a peak difference of ΔE_p = (+235 ± 12) mV

vs. Ag/AgCl, and the midpoint potential slight shift from (-41 ± 4) mV vs. Ag/AgCl to (-17 ± 5) mV vs. Ag/AgCl. The analysis of the ratio between i_p^a after and i_p^a before glucose addition, with the glucose concentration is observed, in Fig. 7.

It is important to highlight that glucose promotes higher anodic current peaks, promoting the oxidation of NADH to NAD$^+$. So glucose interferes with the oxidation of this cofactor. This mechanism may occur in biological systems to facilitate the oxidation process in the absence of an enzyme. But it is a problem for constructing biosensors, because if the electrodes use enzyme which need the redox system NADH/NAD$^+$ as a cofactor, it may sense glucose and not the specific substrate. Also, this may interfere with glucose detection, as NADH reacts with glucose, and diminishes artificially his quantity.

The oxidation of NADH signal was also analyzed in the presence of an eletroactive species, the ascorbic acid at pH 7. For concentration above between 0.75 mM and 12 mM the voltammograms profile did not change. The difference between potential peaks, ΔE_p, before the addition, (233 ± 7) mV, was similar to the one obtained after the addition, (228 ± 15) mV. But they change the formal potential from (-35 ± 7) mV to (-17 ± 1) mV, as the cathodic peak potential becomes more positive E_p^a = (+100 ± 4) mV, and the cathodic peak remains near (-135 ± 8) mV. The oxidation current peak did not change significantly.

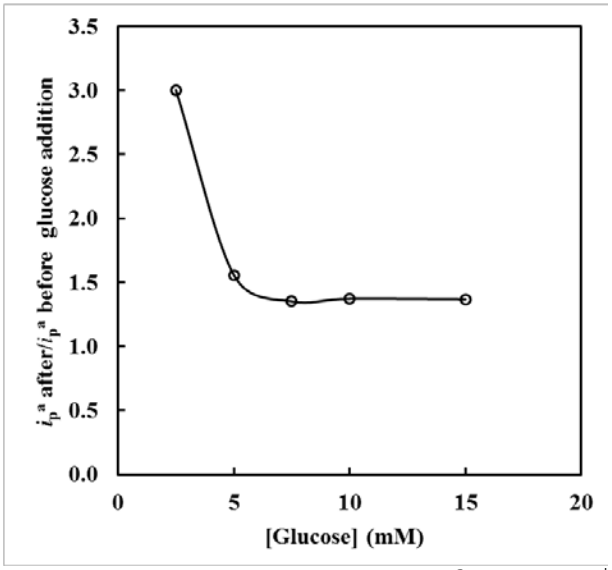

Fig. 7 Variations of the relation between i_p^a NADH/NAD$^+$ signal after and before the glucose addition with the glucose concentration. Cyclic voltammograms recorded at 35 mV/s in PBS buffer (pH 7) with KCl (0.1 M). Each point is the average of two measurements with different sensors.

The NADH signal was also analyzed, at pH 7, in the presence of β-3- HBDH (hydroxybutyrate dehydrogenase), an enzyme that has as cofactor NAD$^+$/NADH, and β-3-HB (hydroxybutyrate).

To do this study, first, a drop of electrolyte (2 μL) was placed in the sensor working area, and recorded cyclic voltammograms in scan rate between 10-100 mV·s^{-1}. Analysis to the cyclic voltammograms shows that the NADH behaves as a quasi-reversible system, as expected. The voltammetric signal (using three different sensors: n=3) is characterized by ΔE_p= (240 ± 8) mV vs. Ag/AgCl a formal potential of $E^{0'}$ = (-38 ± 8) mV vs. Ag/AgCl. After that, a drop ((2 μL) of HBH enzyme solution (0.5 mg/mL), prepared with the electrolyte, was added to the working area. The signal shape did not change, but the anodic current peak diminishes slightly to scan rates lower them 50 mV·s^{-1}, and the ΔE_p obtained was (227 ± 2) mV vs. Ag/AgCl (n = 3), the formal potential of (-8 ± 15) mV vs. Ag/AgCl (n = 3) was obtained. The reduction of the anodic currents may be explained due to the incorporation of the cofactor (NAD$^+$) in the enzyme, with the consequent decrease of NAD$^+$ formed near the electrode surface**.** And the formal potential alteration may be related to the vicinity of the NAD/NAD$^+$ system in this condition and the presence of the enzyme near the electrode surface.

The addition of HB (10 mM) solution, the enzyme catalytic substrate, to the electrode with HBH added by casting, cause an increase in the anodic current, but the cathodic current did not sense the presence of HBH or HB.

The addition of glucose (10 mM) to the working area after the addition of HBH by casting and the subsequent electrochemical analysis revealed also an

increase in the anodic current, but also a change in the $E^{0'}$ to positive values (+6 ± 10) mV vs. Ag/AgCl (n = 3)) and a typical ΔE_p = (+229.0 ± 14) mV vs. Ag/AgCl (n = 3).

4. Conclusions

In this work, we used a simple procedure to fabricate a paper device, using wax to limit the hydrophobic and hydrophilic areas of the biosensor. We immobilized the cofactor in the matrix of the working electrode, which was printed on paper. This procedure is easy and quick, and does not need any drastic treatment.

In this work, the electrode electrochemical reaction is a complex process, and has many challenges. One of them is the increase of the rate of electron transfer between the electrode and NAD/NADH system. This velocity depends not only on the electron transfer, but also on mass transport velocity.

By comparison of the mass transport velocity and charge transference it is possible to identify a quasi-reversible reaction where the electrode process is governed by kinetics and diffusion. In all situations analyzed in this work the system behaved as a quasi-reversible. Some characteristics observed here were attributed to the nature of the electrode (screen-printing) that conditioned kinetics and reduced the mass transport velocity, which can be perceived in the peak-to-peak separation. One strategy used by some researcher is the utilization a solution of 3-APDES (aminopropyldimethly ethoxysilane) prepared with water to improve the hydrophilicity of the electrode surface (graphite) and of the paper channel and enhance the electron transfer velocity [42].

It is important to highlight that even with these obstacles, it was possible to obtain the oxidation and reduction well defined NAD$^+$/NADH signal that was not reported in the literature. It was also possible to test this sensor with non-electroactive molecules such as glucose, and with eletroactive species as ascorbic acid, which shows its versatility. The first one interacts with the electrode and promotes higher oxidation currents, but the ascorbic acid did not interfere with the electrochemical signal.

In future researches it will be interesting to use this approach, and incorporate enzymes relevant to health and to the environment, in the carbon ink, to detect there subtracts. It will be also important using the screen-printing technique and the capability of NAD$^+$/NADH interaction with glucose to develop cheaper biofuel cell.

References

[1] Sekretaryova, A., Eriksson, M., and Turner, A. 2016. "Bioelectrocatalytic Systems for Health Applications." *Biotechnology Advances* 34: 177-97.

[2] Wooten, M., and Gorski, W. 2010. "Facilitation of NADH Electro-Oxidation at Treated Carbon Nanotubes." *Anal. Chem*. 82: 1299. doi: 10.1021/ac902301b

[3] Álvarez-González, I., Saidman, S., Lobo-Castañón, M. J., Miranda-Ordieres, A. Tuñón-Blanco, P. 2000. "Electrocatalytic Detection of NADH and Glycerol by NAD(+)-Modified Carbon Electrodes." *Anal. Chem.* 72: 520-7.

[4] Govindhan, M., Amiri, M., and Chen, A. 2015. "Au Nanoparticle/Graphene Nanocomposite as a Platform for the Sensitive Detection of NADH in Human Urine" *Biosensors and Bioelectronics* 66: 474-80.

[5] Radoi, A., and Compagnone, D. 2009. "Recent Advances in NADH Electrochemical Sensing Design." *Bioeletrochemistry* 76: 126-34.

[6] Ali, I., and Omanovic, S. 2013. "Kinetics of Electrochemical Reduction of NAD$^+$ on a Glassy Carbon Electrode." *Int. J. Electrochem. Sci*. 8: 4283-304.

[7] Hughes, G., Pemberton, R., Fielden, P., and Hart, J. 2015. "Development of a Novel Reagentless, Screen-Printed Amperometric Biosensor Based on Glutamate Dehydrogenase and NAD$^+$, Integrated with Multi-walled Carbon Nanotubes for the Determination of Glutamate in Food and Clinical Applications." *Sensors and Actuators B* 216: 614-21.

[8] Katekawa, E., Maximiano, F., Rodrigues, L., Delbem, M., and Serrano, S. 1999. "Electrochemical Oxidation of NADH at a Bare Glassy Carbon Electrode in Different Supporting Electrolytes." *Analytica Chimica Acta* 385: 345-52.

[9] Saleh, F., Rahman, M., Okajima, T., Mao, L., and Ohsaka, T. 2011. "Determination of Formal Potential of NADH/NAD$^+$ Redox Couple and Catalytic Oxidation of NADH Using Poly (Phenosafranin)-Modified Carbon Electrodes." *Bioeletrochemistry* 80: 121-7.

[10] Gorton, L., and Domınguez, E. 2002. "Electrocatalytic Oxidation of NAD (P)/H at Mediator Modified Electrodes." *Reviews in Molecular Biotechnology* 82: 371-92.

[11] Popescu, I., Domínguez, E., Narváez, A., Pavlov, V., and Katakis, I. 1999. "Electrocatalytic Oxidation of NADH at Graphite Electrodes Modified with Osmium Phenanthrolinedione." *Journal of Electroanalytical Chemistry* 464: 208-14.

[12] Prieto-Simón, B., and Fàbregas, E. 2004. "Comparative Study of Electron Mediators Used in the Electrochemical Oxidation of NADH." *Biosensors and Bioelectronics* 19: 1131-8.

[13] Zhou, j. L., Nie, P. P., Zheng, H, T., and Zhang. J. M. 2009. "Progress of Electrochemical Biosensors Based on Nicotinamide Adenine Dinucleotide (Phosphate)-Dependent Dehyfrogenases." *Chinese Journal of Analytical Chemistry* 37: 617-23.

[14] Zanardi, C., Ferrari, E., Pigani, F., and Seeber, R. 2015. "Development of an Electrochemical Sensor for NADH Determination Based on a Caffeic Acid Redox Mediator Supported on Carbon Black." *Chemosensors* 3: 118-28.

[15] Eguílaz, M., Gutierrez, F., González-Domínguez, J., Matínez, M., and Rivas, G. 2016. "Single-Walled Carbon Nanotubes Covalently Functionalized with Polytyrosine: A New Material for the Development of NADH-Based Biosensors." *Biosensors and Bioeletronics* 86: 308-14.

[16] Friedl, J., and Stimming, U. 2017. "Determining Electron Transfer Kinetics at Porous Electrodes." *Electrochimica Acta* 227: 235-45.

[17] Balamurugan, A., Ho, K-C., Chen, S-M., and Huang, T-Y. 2010. "Electrochemical Sensing of NADH Based on Meldola Blue Immobilized Silver Nanoparticle-Conducting Polymer Electrode." *Colloids and Surfaces A: Physicochem. Eng. Aspects* 362: 1-7.

[18] Lates, V., Gligor, D., Muresan, L., and Popescu, I. 2011. "Comparative Investigation of NADH Electrooxidation at Graphite Electrcdes Modified with Two New Phenothiezine Derivatives." *J. Electroanal. Chem*. 661: 192-7.

[19] Tan, B., Hickey, D., Milton, R., Giroud, F., and Minteer, S. 2015. "Regeneration of the NADH Cofactor by a Rhodium Complex Immobilized on Multi-walled Carbon Nanotubes." *Journal of the Electrochemical Society* 162: H102-7.

[20] Kumar, S., and Cheng, S-M. 2008. "Electroanalysis of NADH Using Conducting and Redox Active Polymer/Carbon Nanotubes Modified Electrodes—A Review." *Sensors* 8: 739-66.

[21] Radoi, A., Compagnone, D., Devic, E., and Palleschi, G. 2007. "Low Potential Detection of NADH with Prussian Blue Bulk Modified Screen-Printed Electrodes and Recombinant NADH Oxidase from Thermus Thermophilus." *Sensors and Actuators B* 121: 501-6.

[22] Rivas, G., Rubianes, M., Rodríguez, M., Ferreyra, N., Luque, G., Pedano, M., Miscoria, S., and Parrado, C. 2007. "Carbon Nanotubes for Electrochemical Biosensing." *Talanta* 74: 291-307.

[23] Arvinte, A., Valentini, F., Radoi, A., Arduiini, F., Tamburri, E., Rotariu, L., Palleshi, G., and Bala, C. 2007. "The NADH Electrochemical Detection Performed at Carbon. Nanofibers Modified Glassy Carbon Electrode. Electroanalysis." *Electroanalysis* 19: 1455-9.

[24] Vasilescu. A., Andressscu, S., Bala, C., Litescu, S., Noguer, T., and Marty, J-L. 2003. "Screen-Printed Electrodes with Electropolymerized Meldola Blue as Versatile Detectors in Biosensors." *Biosensors and Bioelectronics* 18: 781-90.

[25] Doumèche, B., and Blum, L. 2010. "NADH oxidAtion on Screen-Printed Electrode Modified with a New Phenothiazine Diazonium Salt." *Electrochemistry Communications* 12: 1398-402.

[26] Taleat, Z., Khoshroo, A., and Mazloum-Ardakani, M. 2014. "Screen-Printed Electrodes for Biosensing: A Review (2008-2013)." *Microchim Acta* 181: 865-91.

[27] Sahin, M., and Ayranci, E. 2015. "Electrooxidation of NADH on Modified Screen-Printed Electrodes: Effects of Conducting Polymer and Nanomaterials." *Electrochimica Acta* 166: 261-70.

[28] Ensafi, A., Alinajafi, H., Jafari.Asl, M., Rezaei, B., and Ghazaei, F. 2016. "Cobalt Ferrite Nanoparticles Decorated on Exfoliated Graphene Oxide, Application for Amperometric Determination of NADH and H_2O_2." *Materials Science and Engineering C* 60: 276-84.

[29] Gurban, A., Noguer, T., Bala, C., and Rotariu, L. 2008. "Improvement of NADH Detection Using Prussian Blue Modified Screen-Printed Electrodes and Different Strategies of Immobilisation." *Sensors and Actuators B* 128: 536-44.

[30] Avramescu, A., Andreescu, S., Noguer, T., Bala, C., Andreescu, D., and Marty, J-L. 2002. "Biosensors Designed for Environmental and Food Quality Control Based on Screen-Printed Graphite Electrodes with Different Configurations." *Anal. Bioanal. Chem.* 374: 25-32.

[31] Blanco, E., Foster, C., Cumba, L., Cramo, D., and Banks, C. 2016. "Can Solvent Induced Surface Modifications Applied to Screen-Printed Platforms Enhance Their Electroanalytical Performance?" *Analyst* 141: 2783-90.

[32] Radoi, A., Compagnone, D., Valcarcel, M., Placidi, P., Materazzi, S., Moscone, D., and Palleschi. G. 2008. "Detection of NADH via Electrocatalytic Oxidation at Single-Walled Carbon Nanotubes Modified with

Variamine Blue." *Electrochimica Acta* 53: 2161-9.

[33] Prieto-Simón, B., Macanás, J., Muñoz, M., and Fàbregas, E. 2007. "Evaluation of Different Mediator-modified Screen-printed Electrodes used in a Flow System as Amperometric Sensors for NADH." *Talanta* 71: 2102-7.

[34] Fang, L., Wang, S-H., and Liu, C-C. 2008. "An Electrochemical Biosensor of the ketone. 3-[beta]-hydroxybutyrate for Potential Diabetic Patient Management." *Sensors and Actuators B* 129: 818-825.

[35] Mohamed, H. 2016. "Data Analysis Strategies for Targeted and Untargeted LC-MS Metabolomic Studies: Overview and Workflow." *Trends in Analytical Chemistry* 82: 1-11.

[36] Nicholson, R. 1965. "Theory and Application of Cyclic Voltammetry for Measurement of Electrode Reaction Kinetics." *Analitical Chemistry* 37 (11): 1351-5.

[37] Santhiago, M., and Kubota, L. 2013. "A New Approach for Paper-Based Analytical Devices with Electrochemical Detection Based on Graphite Pencil Electrodes." *Sensors and Actuators B* 177: 224-30.

[38] Bard, A., and Faulkner, L. 2001. *Electrochemical Methods, Fundamentals and Applications*, 2nd edition. New York: Wiley.

[39] Määtänen, A., Vanamo, U., Ihalainen, P., Pulkkinen, P., Tenhu, H., Bobacka, J., and Peltonen, J. 2013. "A Low-Cost Paper-Based Inkjet-Printed Platform for Electrochemical Analyses." *Sensors and Actuators B: Chemical* 177: 153-62.

[40] Wang, J., Tian, B., Nascimento, V., and Angnes, L. 1998. "Performance of Screen-Printed Carbon Electrodes Fabricated from Different Carbon Inks." *Electrochim Acta A* 43: 3459-65.

[41] Laviron, E. 1974. "Adsorption, Autoinhibition and Autocatalysis in Polarography and in Linear Potential Sweep Voltammetry." *Electroanalytical Chemistry and Interfacial Electrochemistry* 52: 355.

[42] Nie, Z., Deiss, F., Liu, X., Akbulut, O., and Whitesides, G. 2010. "Integration of Paper-Based Microfluidic Devices with Commercial Electrochemical Readers." *Lab. Chip.* 10: 3163-9.